α of the micelles to solubilize picric acid. Clearly, the few eligible micelles may differ from the majority in shape and physical size. The differences may arise due to fluctuations in water content and aggregation number.

(b) Bimodal Solubilization. In this description it is assumed that both the 6-mer and the 14-mer can incorporate HP

$$A_6 + HP \rightleftharpoons A_6{\cdot}HP \quad K_{s1} \tag{13}$$

$$A_{14} + HP \rightleftharpoons A_{14}{\cdot}HP \quad K_{s2} \tag{14}$$

where $A_6{\cdot}HP$ and $A_{14}{\cdot}HP$ are the colored species, with identical spectroscopic properties. Similar to the situation discussed in the preceding section, in order to be able to simulate the experimental results in Figure 4, again one is forced to assume that only a fraction α_1 of A_6 and a fraction α_2 of A_{14} are eligible for solubilization. Then, equations can be written for K_{s1} and K_{s2}, as well as for $[A_6{\cdot}HP]$ and $[A_{14}{\cdot}HP]$, similar to eq 10 and 11, respectively. The solid curve in Figure 4 was computed by using the optimal values of the adjustable parameters that are summarized in Table III. An equally good fit can be obtained if one assumes $\alpha_1 = \alpha_2$, but such a condition is difficult to justify physically.

Alternate models, in which the idea of fractional eligibility for solubilization is substituted by other hypotheses, were also tested, unsuccessfully. For example, none of the following assumptions or combinations thereof leads to acceptable results: (i) only one type of micelle, the 6-mer or the 14-mer, can solubilize HP; (ii) both types can solubilize picric acid, but only one of the products, $A_6{\cdot}HP$ or $A_{14}{\cdot}HP$, contributes to the optical absorption in the visible range; (iii) both micelle types can solubilize HP, but an indicator-induced micelle formation (eq 15) takes place simul-

$$lA + HP \rightleftharpoons A_l{\cdot}HP \tag{15}$$

taneously, where $l \neq m,n$; (iv) the solubilization process involves the substitution of HP for a surfactant monomer (e.g., eq 16).

$$A_m + HP \rightleftharpoons A_{m-1}{\cdot}HP + A \tag{16}$$

With reference to the optimal values of the parameters found for the bimodal solubilization model (Table III), the results indicate that picric acid is more stable in the 14-mer than in the 6-mer ($K_{s1} \ll K_{s2}$) and that a larger fraction of the 14-mer is eligible for solubilization than the 6-mer ($\alpha_1 < \alpha_2$).

Summary

The investigation of Aerosol-OT reversed micelle in benzene reveals that the equilibrium behavior of the system can be best characterized either by an empirical description as a monomer (single) micelle association (where the mean aggregation number of the micelle is $\bar{n} = 11.6$) or by a bimodal monomer-6-mer-14-mer equilibrium model. The experimental results indicate that, in agreement with findings on similar systems,[11a] aggregation starts already at surfactant concentrations as low as 10^{-6}-10^{-5} M. According to the empirical description, the monomer concentration has a constant value of $[A]_o = 4 \times 10^{-4}$ M at surfactant concentrations of $C_{AOT} \geq 10^{-2}$ M. In this picture, $[A]_o$ can be regarded as the operational cmc of the system. The concept of the operational cmc is absent from the bimodal equilibrium model, where the concentration of all species present increases with C_{AOT}. In contrast to the bimodal model, the single micelle description cannot be quantitatively related in a simple way to any association equilibria that may lead to micelle formation.

Either of the two micelle formation models can serve as the basis for the quantitative description of the solubilization of picric acid in AOT-benzene reversed micelles, where only a small fraction of the aggregates is eligible to accept the substrate. The fractional eligibility can be understood in terms of a multidimensional distribution, where only micelles with a certain aggregation number, pool size, and perhaps shape may accommodate picric acid. The solubilization equilibria formally led to expressions that indicate that the solubilization process can be regarded as adsorption of picric acid by the micelle.

Acknowledgment. This work was partially supported by the Robert A. Welch Foundation and the Organized Research Fund of UTA. Acknowledgment is made to the donors of the Petroleum Research Fund, administered by the American Chemical Society, for partial support of this research.

Reversed Micelle of Aerosol-OT in Benzene. 3. Dynamics of the Solubilization of Picric Acid[1,2]

Kiyoshi Tamura[3] and Z. A. Schelly*

Contribution from the Department of Chemistry, The University of Texas at Arlington, Arlington, Texas 76019. *Received August 7, 1980*

Abstract: Concentration-jump kinetic results on the penetration of picric acid probe molecules into reversed micelles of Aerosol-OT in benzene (containing 0.03% w/w water) reveal the presence of at least four distinct rate processes. One of the relaxation times is in the submillisecond and the others are in the millisecond range. A physical interpretation is presented which is in agreement with the equilibrium descriptions of the system. The formal kinetic treatment allows the computation of the rate parameters which provide the best fit with the experimental results. Numerical values of most of the rate and equilibrium constants involved are reported.

In a recent paper,[1] we reported preliminary results on the kinetics of the penetration of picric acid probe molecule into reversed micelle of Aerosol-OT in benzene. Aerosol-OT (AOT, bis(2-ethylhexyl) sodium sulfosuccinate) is a typical anionic surfactant that forms reversed micelle in apolar solvents. Reversed micelles can be characterized as aggregates of amphiphilic molecules, with their polar head groups concentrated in the interior of the aggregates while their hydrophobic groups extend into the surrounding apolar solvent. The polar head groups may dip into a water pool that usually forms the core of the micelle. Either the water originates from the solvent (where a small amount remains even after careful drying) or it is added on purpose.

Picric acid is colorless in benzene, but it turns yellow when it reaches the polar interior of the reversed micelle after mixing.

(1) Part 1: Tamura, K.; Schelly, Z. A. *J. Am. Chem. Soc.* **1979**, *101* 7643-7644.
(2) Part 2: Tamura, K.; Schelly, Z. A. *J. Am. Chem. Soc.*, preceding paper in this issue.
(3) R. A. Welch Postdoctoral Fellow. On leave of absence from the National Defense Academy, Yokosuka, Japan.

0002-7863/81/1503-1018$01.25/0

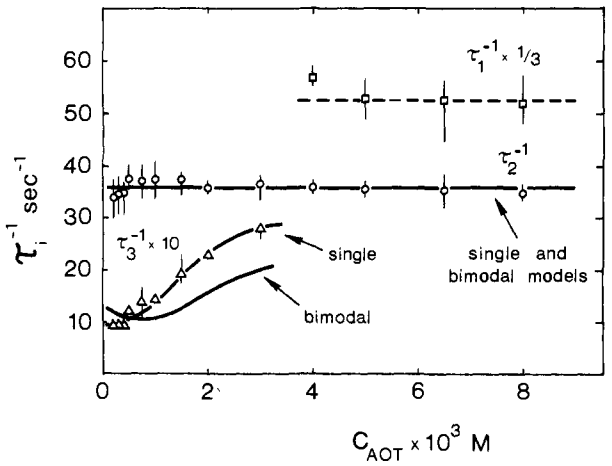

Figure 1. Dependence of the reciprocal relaxation times τ_i^{-1} on the surfactant concentration C_{AOT} at 25 °C and $C_{HP} = 10^{-5}$ M: □, $\tau^{-1}/3$; ○, τ_2^{-1}; △, $10\tau_3^{-1}$. Each point represents the mean value of the data obtained in at least five repeated experiments. The simulated values of τ_i^{-1} are given by the solid curves. The dashed line for τ_1^{-1} is the experimental one. The concentrations are given for after mixing.

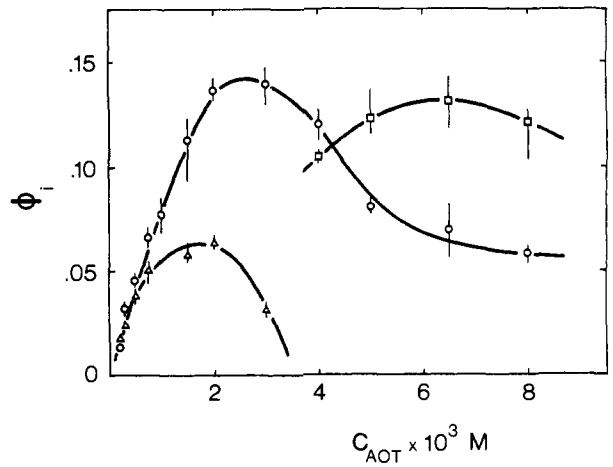

Figure 2. Relaxation signal amplitudes ϕ_i as a function of C_{AOT} at 25 °C and $C_{HP} = 10^{-5}$ M: □, ϕ_1; ○, ϕ_2; △, ϕ_3.

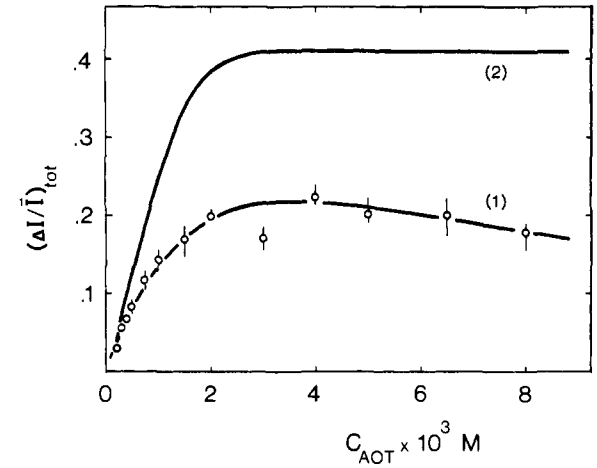

Figure 3. Total relaxation amplitude vs. C_{AOT} at 25 °C and $C_{HP} = 10^{-5}$ M: (1) sum of the three relaxation amplitudes observed, i.e., $\sum_{i=1}^{3}\phi_i$; (2) the total signal amplitude expected from the absorption change on mixing the solutions (calculated by using eq 2).

Monitoring the spectral change allows the investigation of the dynamics of the penetration of the probe into the aggregate. Further extensive kinetic studies have revealed that at least four distinct rate processes characterize the solubilization of the probe by AOT micelles, two more than we originally reported.[1] For the interpretation of the results, a comprehensive equilibrium study of the system had to be undertaken, which is discussed in the preceding paper.[2]

In the present work the detailed analysis of the dynamics of the solubilization of picric acid by AOT reversed micelle in benzene (containing 0.03% w/w water) is discussed. The analysis is based on the equilibrium description[2] of the micelle formation and the solubilization.

Experimental Section

Chemicals. The surfactant Aerosol-OT, the solvent benzene, and the picric acid indicator were purified as reported previously.[1,2] All other chemicals were reagent grade.

Apparatus. The stopped-flow apparatus used, equipped with a 2-cm path length observation cell, has already been described.[4] To improve vibrational insulation of the light source from the stopping shock as well as to simplify the optical alignment procedure, we introduced a glass-fiber optic light pipe between the monochromator and the observation cell. Since the analyzing light beam is not collimated as it passes through the observation cell and the reciprocal linear dispersion of the instrument is different from that of typical recording spectrophotometers, the effective path length $\bar{l}$ of the observation cell (1.38 cm) is different from its physical value (2 cm). This fact is important when absorbances measured on the stopped-flow apparatus are compared with those obtained on spectrophotometers. At a driving pressure of 5 atm and at a mixing volume ratio of 1:1, the dead time of the instrument is 1 ms. The solution reservoirs, sample syringes, and the observation cell were thermostated at 25 ± 0.1 °C.

Results and Discussion

Several different types of concentration-jump[5] and solvent-jump[5] experiments were carried out, the results of each of which contributed to the illumination of the mechanism.

Concentration-Jump Experiments (Type I). Picric acid in benzene (2.0×10^{-5} M) was rapidly mixed with an AOT–benzene solution. The decrease of the transmitted light intensity at λ = 422 nm (which corresponds to an absorption peak of the final solution[2]) was monitored on the oscilloscope. All the oscilloscope traces observed (including the ones of the type II experiments in the next section) could be represented by a sum of exponentials,

from which the relaxation time τ_i and relaxation signal amplitude ϕ_i of the individual processes i were obtained. The two quantities are related by eq 1 where $\bar{I}$ is the transmitted light intensity $I(t)$

$$\Delta I/\bar{I} = \sum_i \phi_i \exp(-t/\tau_i) \qquad (1)$$

at the final equilibrium and ΔI is the deviation of $I(t)$ from $\bar{I}$ (i.e., $\Delta I = I(t) - \bar{I}$).

Figures 1 and 2 show the reciprocal relaxation times τ_i^{-1} and ϕ_i as a function of the surfactant concentration C_{AOT} (after mixing), respectively. The change of the picric acid concentration in the range of $(0.5–1.0) \times 10^{-5}$ M has no effect on τ_i. The fastest of the three processes shown (τ_1) can be observed only at $C_{AOT} \geq 4 \times 10^{-3}$ M, and τ_1^{-1} is practically independent of the surfactant concentration. The signal amplitude ϕ_i has a flat maximum at 6.5×10^{-3} M AOT. The second process is observed over the entire AOT concentration range studied ($(0.2–8) \times 10^{-3}$ M), and τ_2^{-1} is practically independent of C_{AOT}; ϕ_2 has a maximum at $C_{AOT} = 2.5 \times 10^{-3}$ M. The slowest process can be observed only at low surfactant concentrations ($C_{AOT} \leq 3 \times 10^{-3}$ M). The reciprocal relaxation time τ_3^{-1} increases with the AOT concentration, and ϕ_3 has a maximum around $C_{AOT} = 1.8 \times 10^{-3}$ M.

The presence of at least one more process (τ_0), which is too fast for observation by the stopped-flow apparatus, can be conjectured from a comparison of the total observed signal amplitude $\sum_i \phi_i$ with the one that should be expected on mixing the picric acid and AOT solutions. The expected total signal amplitude $(\Delta I/\bar{I})_{tot}$ can be calculated from eq 2 where C_{HP} is the analytical

$$(\Delta I/\bar{I})_{tot} = \exp(2.303\bar{\epsilon}\bar{l}C_{HP}) - 1 \qquad (2)$$

(4) Wong, M. M.; Schelly, Z. A. *Rev. Sci. Instrum.* **1973**, *44*, 1226–1230.
(5) Chao, D. Y.; Schelly, Z. A. *J. Phys. Chem.* **1975**, *79*, 2734–2736. Schelly, Z. A.; Chao, D. Y. *Adv. Mol. Relaxation Interact. Processes* **1979**, *14*, 191–202.

concentration (after mixing) and $\bar{\epsilon}$ is the known apparent molar decadic extinction coefficient[2] of picric acid, respectively; $\bar{l}$ stands for the effective (calibrated) path length of the observation cell of the stopped-flow apparatus. As evident from Figure 3, about half of the total absorption change on mixing takes place too rapidly for observation, during the dead time of the instrument. Besides the four processes discussed, no additional very slow reaction takes place, as tested in long-time experiments up to 1 h.

Concentration-Jump Experiments (Type II). Two AOT–benzene solutions of the same concentration were mixed, where one of the solutions contained also picric acid (2.0×10^{-5} M). Thus, in such experiments only C_{HP} is "jumped". Two relaxations can be observed in the AOT concentration region not higher than 3×10^{-3} M (the absorbance increases with time), while no relaxation is present at higher C_{AOT}. This critical concentration is near the saturation point of the absorption peak height,[2] which in fact presents a clear indication for complete solubilization of all picric acid by the micelles above $C_{AOT} = 3 \times 10^{-3}$ M in one of the solutions, already before mixing. The relaxation times measured (and their concentration dependence) are very similar to τ_2 and τ_3 obtained in the type I experiments, but the signal amplitudes, of course, are less than half of those values of the type I. Since the AOT concentration is kept constant before and after mixing, the kinetic processes observed should be related to the solubilization of HP by the micelles rather than the formation–decomposition process of the micelles.

From the similarity of the results of the type I and II experiments, one may conclude that the kinetic data in Figures 1 and 2 are associated with the solubilization of the picric acid probe into the AOT micelles. In both types of experiments, only an increase of the absorbance with time was observed which corresponds to the increase in concentration of the solubilized indicator. From this fact, as well as from the conclusions of the type II experiments, it follows that the formation–decomposition process of the reversed micelle must reach equilibrium much more rapidly[6] than the solubilization process. If the opposite were true, the absorbance should have decreased in the type I experiments, and no relaxation should have been observed in the type II ones.

Solvent-Jump Experiments. Solutions containing both 2.0×10^{-5} M picric acid and 10^{-4}–10^{-2} M AOT were rapidly diluted with pure benzene in the stopped-flow apparatus. The fact that no relaxation could be observed in the time range of 10^{-3}–5 s indicates that the solubilized indicator is too stable to be significantly perturbed by a twofold dilution.[1]

Physical Picture. In order to develop a physical picture of the penetration of picric acid into AOT reversed micelles, we must recall some of the characteristic features of the kinetic and equilibrium[2] results.

(i) There exists a very rapid solubilization step that occurs during the dead time of the stopped-flow experiments.

(ii) The relaxation time τ_2 is constant over the whole AOT concentration range studied. Therefore, it is plausible to consider that the solubilization process involves at least one first-order step.

(iii) The slowest relaxation process (τ_3) disappears at $C_{AOT} \geq 4 \times 10^{-3}$ M, but the fastest process (τ_1) can be observed only in this concentration range. The boundary concentration is clearly above the saturation point where almost all of the picric acid is solubilized by the micelles in the final equilibrium solution.[2]

(iv) As to the species present in the solution and their equilibrium distribution, in the previous equilibrium study we arrived at two possible descriptions of the system. One of them is based on an empirical method, resulting in a single micelle model (with mean aggregation number $\bar{n} = 11.6$). The other one is a bimodal micelle model with two types of aggregates: 6-mer and 14-mer. This model is based on simple aggregation equilibria. Figure 4 shows the population distribution of all (but the monomer AOT) species present at $C_{HP} = 10^{-5}$ M. The individual concentrations were computed on the basis of the bimodal model.

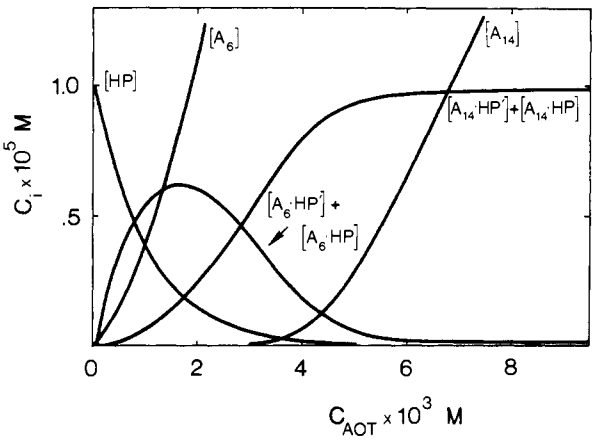

Figure 4. Equilibrium concentrations of the species present in AOT–benzene solution containing 10^{-5} M picric acid at 25 °C: [HP], free picric acid in the bulk solution; [A_6], those free 6-mers which are eligible for solubilization; ([A_6·HP'] + [A_6·HP]), 6-mer containing a picric acid; [A_{14}], those free 14-mers which are eligible for solubilization; ([A_{14}·HP'] + [A_{14}·HP]), 14-mers containing picric acid. See eq 4 and 5 and the subsequent explanation for the identity of the species.

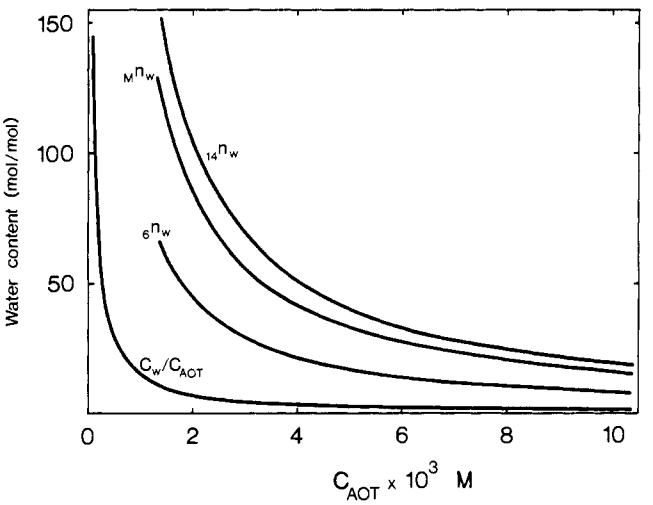

Figure 5. Distribution of water in AOT–benzene solution containing 0.03% w/w water: C_w/C_{AOT}, number of water molecules per AOT molecule (the value of C_w/C_{AOT} is 1 at $C_{AOT} = 14.6 \times 10^{-3}$ M); $_6n_w$ and $_{14}n_w$, average number of water molecules solubilized in the 6-mer and 14-mer, respectively; $_Mn_w$, average number of water molecules per micelle (single micelle model).

(v) Further, we showed that only a small fraction of the micelles (α in the single micelle model, and α_1 for the 6-mer and α_2 for the 14-mer in the bimodal model) is eligible for solubilizing picric acid.

(vi) The solubilization equilibria can be related to a Langmuir-type adsorption isotherm, enabling us to view the solubilization as an adsorption at the interior surface of the reversed micelle.

(vii) Another important characteristic of reversed micelles which must be taken into account is the amount of water solubilized in the micelles, i.e., the size of the water pools.[7] The solvent benzene used contains 0.03% w/w water,[8] which is less than half of the saturation concentration.[9] In AOT–benzene solution the water may be partitioned between the bulk solvent and the pools of the micelles. No quantitative information is available on the parti-

(6) Eicke, H. F.; Hopmann, R. F. W.; Christen, H. *Ber. Bunsenges. Phys. Chem.* **1975**, *79*, 667–673.

(7) Menger, F. M.; Donohue, J. A.; Williams, R. F. *J. Am. Chem. Soc.* **1973**, *95*, 286–288. Menger, F. M.; Saito, G. *Ibid.* **1978**, *100*, 4376–4379.

(8) Herrmann, U.; Schelly, Z. A. *J. Am. Chem. Soc.* **1979**, *101*, 2665–2669.

(9) Énglin, B. A.; Platé, A. F.; Tugolukov, V. M.; Pryanishnikova, M. A. *Khim. Tekhnolog. Topl. Masel* **1965**, *10*, 42–46.

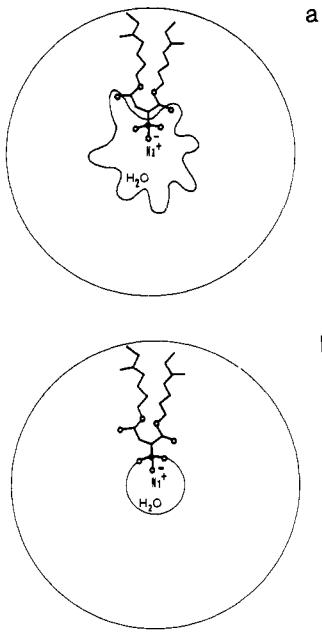

Figure 6. Schematic representation of Aerosol-OT reversed micelle in benzene, showing only one surfactant molecule dipping into the water pool. The open circles symbolize oxygen, and the solid ones sulfur. (a) Dilute solution, $C_{AOT} < 4 \times 10^{-3}$ M; (b) concentrated solution, $C_{AOT} > 4 \times 10^{-3}$ M.

tioning. In order to obtain an estimate of the average pool size as a function of C_{AOT}, one can assume that all the water is incorporated by the micelles, and the water-solubilizing ability of each micelle is proportional to the number of surfactant monomers in the aggregate. Thus, for the bimodal micelle model, the average number of H_2O molecules per 6-mer, ${}_6n_w$, and per 14-mer, ${}_{14}n_w$, is given by eq 3 where C_w and $[A_i]$ are the molar concentrations

$$ {}_6n_w = 6C_w/(6[A_6] + 14[A_{14}]) \qquad {}_{14}n_w = 14C_w/(6[A_6] + 14[A_{14}]) \tag{3} $$

of H_2O and the aggregates, respectively. Figure 5 shows the number of H_2O molecules per AOT molecule C_w/C_{AOT} as well as ${}_6n_w$ and ${}_{14}n_w$ as a function of C_{AOT}. For the single micelle model, the average number of water molecules per micelle M, ${}_Mn_w = C_w/[M]$, is included in the diagram as well. Here, we must notice that the water-solubilization capacity of AOT in hydrocarbons is limited.[10] For example, we found that 0.1 M AOT in benzene cannot solubilize more than between 1.1 and 2.2 M of water. The curves in Figure 5 were constructed with provision to the solubilization limit.

With the consideration of the points above, Figure 6 gives a schematic representation of the AOT reversed micelle. On the basis of the information available, a physical picture of the solubilization evolves which can be consolidated with either of the two micelle models, with only slight modifications. In dilute AOT solution (below $C_{AOT} \approx 4 \times 10^{-3}$ M), apparently there is enough water present to hydrate all polar groups (COO and $SO_4^-Na^+$) of AOT in the micelle (Figure 6a). When picric acid from the bulk solvent penetrates the micelle, the indicator first reaches one of the carboxyl groups, where it adsorbes in a very rapid step. This process may correspond to the first color change[11] (τ_0) that is too fast for observation by the stopped-flow instrument. In a second step, HP moves further into the interior of the micelle, and finally adsorbs at a hydrated sulfonate group of the micelle in the pool. The desorption–adsorption process involved is assumed to be slow. The two slower relaxations, τ_2 and τ_3, may be associated with this step, with respect to the penetration of the 14-mer and 6-mer for the bimodal micelle model. If the empirical single micelle model is used, some alteration of the formal mechanism is required (see the section on Semiquantitative Formal Treatments for details), which, however, does not change the course of events for the probe.

At AOT concentrations above 4×10^{-3} M, with the shrinkage of the pool size (Figure 5), there is not enough water present any more to hydrate all of the polar groups in the micelle. Consequently, part of the carboxyl groups are dehydrated (Figure 6b). When the HP and AOT solutions are mixed, some of the picric acid rapidly adsorbs to those carboxyl groups which still possess hydrate water (τ_0). But then, the replenishment of the water pools becomes rate determining. The H_2O content of the picric acid solution becomes the source of water for the micelles, after the solutions are mixed. Thus, in the second step, the rate-determining process of the color change is the solubilization of water from the bulk solvent into the micelles. The fastest relaxation observed (τ_1) may be associated with this step. Indeed, the τ_1 process is actually a slowed-down version of the τ_0 process. Such an assignment for τ_1 is supported by the fact that at high surfactant concentrations the fast relaxation disappears if the water content of the AOT solution is increased already before mixing with HP. Also, the rate of penetration of water into the micelle compares reasonably with the much slower water transport across vesicle bilayers.[12]

Semiquantitative Formal Treatments. Without the knowledge of the actual distribution of the aggregation numbers and the water content of the micelles, several approximations must be made to obtain numerical values for the rate parameters involved in the processes τ_2 and τ_3. On the basis of the arguments of the previous section, the simplest reaction schemes are presented which are in agreement with the single and the bimodal micelle models. So that the number of adjustable parameters could be minimized, as a first approximation, ordinary linearized relaxation treatment is used, although the concentration-jump perturbation in our experiments is not strictly small.

(i) Bimodal Micelle Model. With reference to the equilibrium results[2] and the physical picture developed, the penetration of the 6-mer and 14-mer by HP can be written as eq 4 and 5, where HP

$$ A_6 + HP \overset{K_{o1}}{\rightleftharpoons} A_6{\cdot}HP' \underset{k_{-1}}{\overset{k_1}{\rightleftharpoons}} A_6{\cdot}HP \tag{4} $$

$$ A_{14} + HP \overset{K_{o2}}{\rightleftharpoons} A_{14}{\cdot}HP' \underset{k_{-2}}{\overset{k_2}{\rightleftharpoons}} A_{14}{\cdot}HP \tag{5} $$

is the free picric acid in the bulk solution, A_i are the aggregates *eligible* for the solubilization of the probe, $A_f{\cdot}HP'$ represents the micelles with picric acid adsorbed at a carboxyl group of AOT, and $A_f{\cdot}HP$ represents the ones with HP adsorbed at a sulfonate group.[13] The first steps in eq 4 and 5 are considered very rapid (τ_0; and in the high concentration range also τ_1) and to be in equilibrium at all times as compared with subsequent steps. Since the solubilization has been shown analogous to the Langmuir-type adsorption,[2] it is assumed that the entrance of the probe into the micelle does not shift the micellization equilibria. Since the concentration maximum of the total of $A_6{\cdot}HP$ plus $A_6{\cdot}HP'$ (Figure 4) is the same AOT concentration range where the slowest relaxation occurs (Figures 1 and 2), τ_3 is ascribed to process 4 and τ_2 to process 5. Because of the observed concentration dependence of τ_3, it is reasonable to assume that the concentration of $A_6{\cdot}HP'$ is much lower than that of $A_6{\cdot}HP$ and can be ignored compared with the latter.

(10) Frank, S. G.; Zografi, G., *J. Colloid Interface Sci.* **1969**, *29*, 27–35.

(11) In order to reconcile the new kinetic and equilibrium spectrophotometric[2] results, we have to revise our previous assumption[1] about the spectral properties of the indicator attached to a COO group of the micelle. The species is symbolized by DMs in ref 1 and by $M{\cdot}HP'$ or $A_f{\cdot}HP'$ in the present work. Now, the complex is assumed to be colored, with the same spectral properties as HP adsorbed further inside at the interface of the pool of the micelle ($M{\cdot}HP$ or $A_f{\cdot}HP$).

(12) Lawaczeck, R. *Ber. Bunsenges. Phys. Chem.* **1978**, *82*, 930. Penetration of water into the AOT reversed micelle is ca. 50 times as fast as that across lipid vesicle bilayers.

(13) In ref 2 we did not have to distinguish between $A_f{\cdot}HP$ and $A_f{\cdot}HP'$; hence, only the unprimed symbol was used for the *collection* of the two species.

Table I. Kinetic Parameters for the Solubilization of Picric Acid into Aerosol-OT Reversed Micelles

(i) Bimodal Micelle Model[a]			
$K_{o1}k_1$, M^{-1} s^{-1}	10^6	k_2, s^{-1}	9.6
k_{-1}, s^{-1}	2.8	k_{-2}, s^{-1}	26
K_{o2}, M^{-1}	5.6×10^7		
(ii) Single Micelle Description[b]			
k_1, s^{-1}	2.3	k_2, s^{-1}	2.4
k_{-1}, s^{-1}	0.9	k_{-2}, s^{-1}	34
K_{o2}, M^{-1}	2.3×10^6		

[a] The equilibrium parameters used are as follows[2]: $\alpha_1 = 0.064$; $\alpha_2 = 0.095$; $K_{s_1} = 3.6 \times 10^5$; and $K_{s_2} = 7.7 \times 10^7$. [b] The equilibrium parameters used are[2] $\alpha = 0.10$ and $K_s = 6.8 \times 10^5$.

From the above reaction scheme, the rate equations are given by eq 6. After linearization by the usual procedure, the relaxation

$$d[A_6{\cdot}HP]/dt = K_{o1}k_1[A_6][HP] - k_{-1}[A_6{\cdot}HP]$$
$$d[A_{14}{\cdot}HP]/dt = k_2[A_{14}{\cdot}HP'] - k_{-2}[A_{14}{\cdot}HP] \quad (6)$$

times are given by

$$1/\tau = (a_{11} + a_{22})/2 \pm [[(a_{11} - a_{22})/2]^2 + a_{12}a_{21}]^{1/2} \quad (7)$$

where

$$a_{11} = K_{o1}k_1[A_6](1 + K_{o2}[HP])/(1 + s) + k_{-1}$$
$$a_{12} = K_{o1}k_1[A_6]/(1 + s)$$
$$a_{21} = K_{o2}k_2[A_{14}]/(1 + s)$$
$$a_{22} = k_2 s/(1 + s) + k_{-2} \quad (8)$$

with

$$s = K_{o2}([A_{14}] + [HP]) \quad (9)$$

From the equilibrium relations, the known solubilization constants[2] K_{s1} and K_{s2} can be expressed as

$$K_{s1} = K_{o1}(1 + k_1/k_{-1}) \approx K_{o1}k_1/k_{-1}$$
$$K_{s2} = K_{o2}(1 + k_2/k_{-2}) \quad (10)$$

where the approximation $k_1/k_{-1} \gg 1$ corresponds to the low concentration assumed for $A_6{\cdot}HP'$. Thus, the relaxation times τ_2 and τ_3 can be calculated from eq 7–10 with the use of assumed values of K_{o2}, $K_{o1}k_1$, and k_2. If the adjustable parameters are optimized by minimizing the relative standard deviation between the observed and computed values of the relaxation times, the solid curves in Figure 1 are obtained. The fit is excellent for τ_2^{-1}, and, considering the simplicity of the assumed mechanism and the approximations involved, acceptable for τ_3^{-1}. Table I summarizes the kinetic parameters obtained together with the equilibrium parameters used in the computations.

(ii) Single Micelle Description. The simplest and most plausible solubilization scheme to interpret τ_2 and τ_3 by this micelle model can formally be written as

$$M' \underset{k_{-1}}{\overset{k_1}{\rightleftharpoons}} M \quad (11)$$

$$M' + HP \overset{K_{o2}}{\rightleftharpoons} M{\cdot}HP' \underset{k_{-2}}{\overset{k_2}{\rightleftharpoons}} M{\cdot}HP \quad (12)$$

In eq 11 and 12 both M′ and M are micelles *eligible* to solubilize picric acid. However, M′ is assumed to be penetrable much more rapidly than M. The reason for this may be a difference in actual aggregation number or pool size. M·HP′ and M·HP are micelles in which HP is adsorbed at the carboxyl and sulfonate groups, respectively. Similar to the bimodal case, the first step in eq 12 is assumed to be very rapid (τ_0; and in the high concentration range also τ_1) in comparison to the other reactions. The coupled rate equations are given by

$$d[M]/dt = k_1[M'] - k_{-1}[M] \quad (13)$$
$$d[M{\cdot}HP]/dt = k_2[M{\cdot}HP'] - k_{-2}[M{\cdot}HP] \quad (14)$$

Again, the linearized relaxation treatment results in two relaxation times (τ_2 and τ_3) expressed by eq 7. Here, the a_{ij} terms are the following:

$$a_{11} = k_1(1 + K_{o2}[M'])/(1 + s) + k_{-1}$$
$$a_{12} = k_1/(1 + s)$$
$$a_{21} = k_2K_{o2}[HP]/(1 + s)$$
$$a_{22} = k_2 s/(1 + s) + k_{-2} \quad (15)$$

with

$$s = K_{o2}([M'] + [HP]) \quad (16)$$

The relaxation times τ_2 and τ_3 may be associated with the reactions 11 and 12, respectively. In this reaction scheme, the known solubilization constant[2] K_s can be expressed as

$$K_s = K_{o2}(1 + k_2/k_{-2})/(1 + k_1/k_{-1}) \quad (17)$$

The reciprocal relaxation times τ_2^{-1} and τ_3^{-1} can be simulated by using eq 7 and 15–17 and with the four rate constants $k_{\pm i}$ in (11) and (12) as adjustable parameters. The computational procedure is the same as described in the previous section. Figure 1 shows the calculated values as solid lines. Possibly because of the larger number of adjustable parameters used (four vs. three), the fit achieved for τ_3^{-1} is obviously better with the single micelle model.

Summary

The investigation of the dynamics of solubilization of probe molecules by reversed micelles may contribute to the general understanding of transport processes through more complex membrane structures. The present kinetic study reveals that the penetration of a picric acid indicator into Aerosol-OT reversed micelles in benzene involves at least four distinct steps: one in the submillisecond and three in the millisecond range. The first step (τ_0) may be associated with the adsorption of the probe at a hydrated carboxyl group in the interior of the micelle. The interpretation of the two slower steps τ_2 and τ_3 depends on the micellization model adopted. With the bimodal micelle model, τ_2 can be ascribed to the advancement of the probe to a more polar hydrated sulfonate group site further inside the 14-mer. τ_3 can be ascribed to the same process in the 6-mer. If the theoretically less founded single micelle description is adopted, τ_2 may be associated with the same process inside the micelle as above, and τ_3 with the reequilibration of two types of micelles eligible for solubilization (eq 11). At $C_{AOT} \gtrsim 4 \times 10^{-3}$ M the average pool size seems to decrease to a level where part of the carboxyl groups become dehydrated. After occupation of the still hydrated carboxyl sites by the probe, the replenishment of the pools becomes rate determining for the entrance of the remaining free picric acid into the micelles.

Acknowledgment. This work was partially supported by the Robert A. Welch Foundation and the Organized Research Fund of UTA. Acknowledgment is made to the donors of the Petroleum Research Fund, administered by the American Chemical Society, for partial support of this research.